Nuclear Instruments and Methods in Physics Research A 624 (2010) 549–553

Contents lists available at ScienceDirect

Nuclear Instruments and Methods in Physics Research A

journal homepage: www.elsevier.com/locate/nima

A harmonic coil measurement system based on a dynamic signal acquisition device

J.X. Zhou*, L. Li, B.G. Yin, C.D. Deng, W. Kang, Y. Chen, Z. Zhang, S.N. Fu

Institute of High Energy Physics, P.O. Box 918-9, Beijing 100049, PR China

ARTICLE INFO

Article history:
Received 4 May 2010
Received in revised form
26 September 2010
Accepted 3 October 2010
Available online 13 October 2010

Keywords:
DC and AC magnetic field measurements
Harmonic coil
Dynamic signal acquisition device
Digital bucking

ABSTRACT

A new harmonic coil measurement system based on a dynamic signal acquisition device has been successfully developed to check the field quality of the quadrupole magnet for the CSNS/RCS, which operates at the 25 Hz excitation cycle with a DC bias. It was designed to acquire multiple channels of data with a wide dynamic range of input signals, which are typically generated by a harmonic coil and an encoder. A dedicated algorithm was developed in LabView code to identify over specified intervals, synchronized to the coil's rotation in the magnetic field. Through full integration of hardware and software, the traditional device (PDI 5025) is replaced successfully. This paper summarizes the characteristics of the system and presents the results of DC measurements.

1. Introduction

The under construction project of China Spallation Neutron Source (CSNS) is a large science facility, which can provide users a powerful and comprehensive research platform in many frontier areas. CSNS mainly consists of a linear accelerator, a 1.6 GeV rapid cycling synchrotron (RCS), and a target station [1].

The RCS magnet system mainly consists of 24 dipole magnets, 48 quadrupole magnets, and 16 sextupole magnets, in which the dipole and quadrupole magnets are excited by a 25 Hz alternating current with a DC bias. Field errors of the magnets have a significant impact on the operation of RCS in term of the beam loss control. Also eddy current, vibration, and other characteristics raised from AC current excitation exist in the magnets. To study these issues, a prototype quadrupole magnet for the CSNS/RCS had been fabricated. Its design parameters are listed in Table 1. The magnetic field measurements are needed to verify whether the field quality can meet the RCS accelerator operation requirements. Since the magnet has an aperture radius of 15.4 cm and an effective length of 70 cm, one can expect the large fringe fields [2–4]. Just like the systems in Refs. [5,6], the fringe field of the magnet had been measured by Hall probe measurement system [7] in IHEP. Because of the tune shifts produced by the kinematic corrections is equally important for the CSNS/RCS ring [8–10], the overall effect of high order harmonics along the beam line must be measured, and the measurement precision must be better than 10^{-4}. Meanwhile, the method of magnet end chamfer needed to be applied in order to reduce the high order harmonic components. To meet these requirements, a harmonic coil measurement system has been developed to perform the DC and AC field measurements. Since the magnet has a big aperture, AC current excitation will give rise to eddy current and vibration, which can result in difficulties in the design, fabrication, installation, and alignment of the measurement coil. It was estimated that the biggest dynamic changes of induced voltage inside the harmonic coil is about ± 37 V. Since the traditional acquisition devices (PDI-5025 integrator [11]) does not have the ability to work in a large input range and fast sample mode, a device that can accurately and synchronously sample all the required field signals was considered. A new method that can use the written code with special functions to take role of some circuit or hardware has been adopted. Through the perfect integration with an acquisition device which has large dynamic range, it is more efficient and flexible than developing a new integrator with a large range.

2. Measurement principle

For the DC measurements, the standard radial coil technique has been used [12]. The measurement coil rotates with an angular velocity ω in the magnetic field and $\theta=\delta$ is the angular position at time $t=0$, then $\theta=\omega t+\delta$. The time dependent magnetic flux through the coil is then

$$\Phi(t)=ML_{eff}\sum_{n=1}^{\infty}|C_n|(R_1^n-(-R_3)^n)\cos(n\omega t+n\delta+\theta_n) \quad (1)$$

where M is the coil turns, L_{eff} the effective length of the magnetic field, C_n the complex constant, the integer n is half the number of poles. R_1 and R_3 are the radii of the coil two sides with respect to the rotation axis. The induced voltage inside the coil is sampled and integrated. Since the amplitude of the voltage signal is proportional to the angular velocity, it is essential to control the angular velocity

* Corresponding author. Tel.: +86 10 88236235; fax: +86 10 88236190.
E-mail address: zhoujx@ihep.ac.cn (J.X. Zhou).

0168-9002/$ - see front matter © 2010 Elsevier B.V. All rights reserved.
doi:10.1016/j.nima.2010.10.009

and make corrections for any speed fluctuations. The integrated voltage signal gives the flux, which is independent of angular velocity [13].

3. The components of CSNS/RCS quadrupole magnetic measurement system

3.1. Harmonic coil

The harmonic coil was designed and fabricated in IHEP. In order to obtain a high sensitivity for high order harmonics, we adopted radial coil type (Fig. 1) with bucking structure for the quadrupole magnets [12]. The harmonic coil consists of a main coil (outer coil) and a bucking coil (inner coil), which are located at the plane of (R_1, θ), $(R_3, \theta+\pi)$ and the plane of (R_2, θ), $(R_4, \theta+\pi)$, respectively. The parameters of the measurement coil are listed in Table 2. The magnet fringe field has been considered and the length of the coil is about 2 m that is 4 times the magnet aperture plus its effective length. A color-coded multifilar wire [14] is used for the coil winding. It consists of 20 strands, and each strand is 0.07 mm thick and 50 μm in diameter. The material of the coil framework is fiberglass-reinforced epoxy (G10). After the coil fabrication, an engraved line was marked along the (R_1, θ) direction from the origin to the outside diameter in order to measure the angle between the magnetic field plane and the horizontal plane. The accuracy of the engraved line is about 1 m rad.

3.2. Data acquisition device

Whether the acquired data are accurate and reliable is very important for the system. Using a calibrated voltage source, a series of standard signals are supplied to the input channels of the different acquisition device. After a series of tests, the PXI-4462 [15] dynamic signal acquisition device from National Instruments company is finally selected and the main parameters of it are listed in Table 3. The calibrated voltage source was supplied to one input channel of the PXI-4462 from 0 to 10 V at a step of 0.1 V and the gain for the test channel was set to zero. The test results of PXI-4462 show the standard deviation of every measured voltage in ppm of the input channel, as plotted in Fig. 2. The maximal deviation is less than 12 ppm. The accuracy and linearity of this device are satisfactory.

3.3. Adjustable support platform and control units

In order to reduce the measurement error coming from the magnet eddy current and vibration, each end of the coil is supported by a bracket and then the coil is suspended inside the magnet aperture (see Fig. 3). The master side, the slave side, and the magnet platform can be adjusted to ensure that the center of the measurement coil is in the mechanical center of the quadrupole magnet. The simple control diagram of the measurement system is shown in Fig. 4. The magnet current is controlled by the PXI-6509 device and monitored by Agilent 34401 through DC current transducer. PXI-7354 is a high-precision motor control device, which is used to control three servo motors for their corresponding movement. Two servo motors located at the bracket of the slave side are used to adjust the platform and another servo motor at the master side is used to drive the measuring coil rotating via the drive shaft. A high-resolution annular encoder (8192 resolutions/cycle) is seated on the drive shaft and looped to the PXI-7354 motion control device and the encoder signals are acquired by PXI-4462 at

Table 1
Parameters of CSNS/RCS quadrupole prototype [1].

Aperture diameter (mm)	308
Magnetic field gradient G (T/m)	4.5
Linear deviation of the excitation curve	$<1\%$
Effective length L_{eff} (m)	0.7
Radius of good field region R_0 (mm)	141
Requirements of harmonic errors	$\triangle BL/BL < 8\times10^{-4}$

Table 2
Parameters of the harmonic coil.

R_1 (mm)	130
R_2 (mm)	92.08
R_3 (mm)	97.5
R_4 (mm)	59.58
Main coil turns N_1	80
Bucking coil turns N_2	120

Table 3
Main parameters of PXI-4462 device [15].

input channels	4
A/D converter (ADC) resolution	24 bits
Sample rates (fs)	1–204.8 kS/s
Input signal range (V)	±0.316 to ±42.4 (depending on gain)
Gain	-20, -10, 0, 10, 20, 30

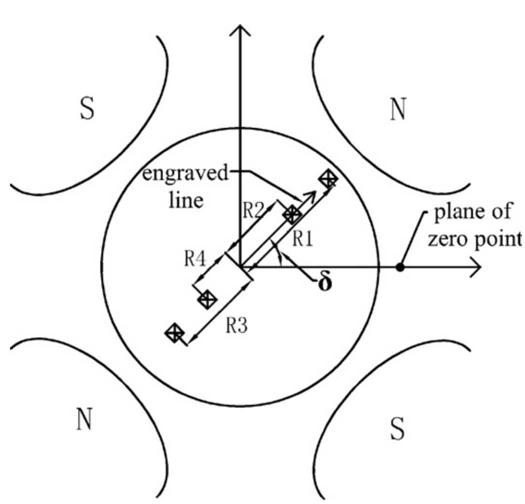

Fig. 1. The geometry of the harmonic coil in quadrupole magnet.

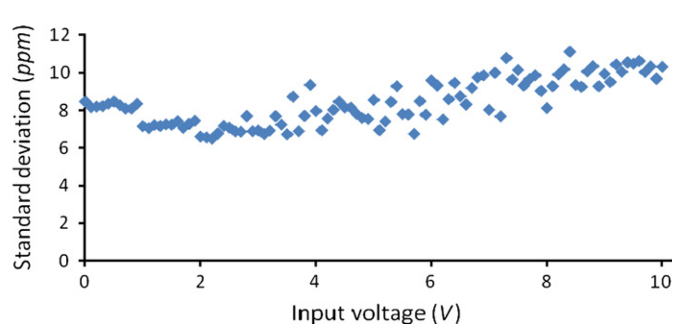

Fig. 2. Standard deviation of PXI-4462 device at different input standard signals.

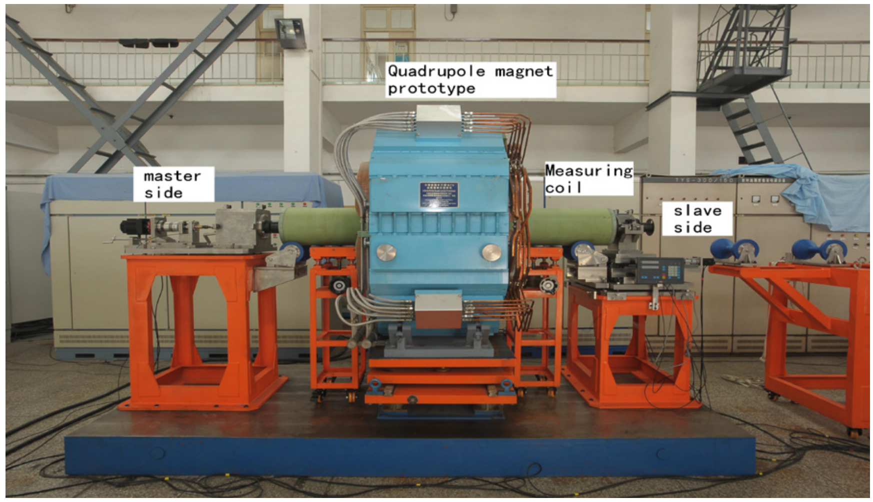

Fig. 3. Support platform of the measurement system.

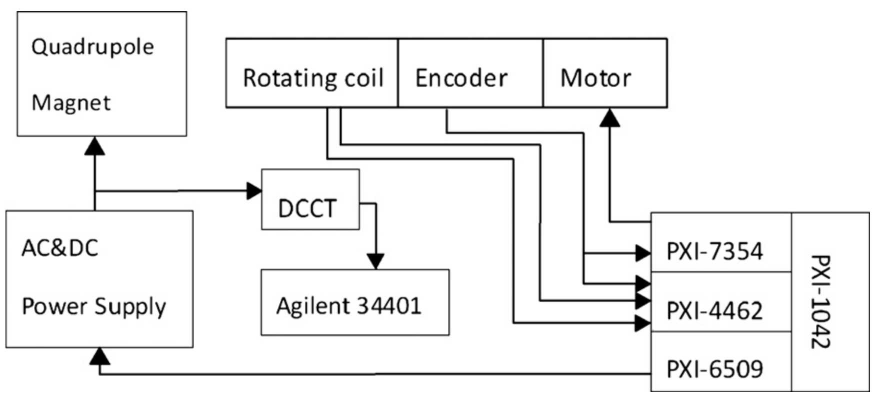

Fig. 4. Simple control diagram of the measurement system.

the same time. These PXI devices are inserted to the different slots of PXI-1042 and communicated with each other through the RTSI buses. The measurement program is written in LabView, which includes controlling the magnet current, identifying the signal of the encoder, displaying of the measurement data, and storing the results automatically.

4. Data acquisition and processing

The motor drives the coil rotating slowly until the engraved line (see Fig. 1) parallel to the plane of zero point (that is $\delta = 0$), which can be checked by an optical instrument. With the confirmed zero point, the angle between the magnetic plane and the horizontal plane can be measured in a high precision. While the coil rotates at the second cycle from the zero point, the induced voltage of the two coils and sequence pulses of encoder are recorded synchronously by three separate channels of the PXI-4462. They are stored into three arrays, which have the same size, and three elements with the same index have been acquired at the same time. So the induced voltage in the two coils at an angular orientation θ can be identified by identifying the 8192 TTL pulse signals of the encoder in one circle. A dedicated LabView code whose schematic layout is shown in Fig. 5 has been written to identify TTL signals from the encoder. Taking the rising edge as the trigger point, 8193 trigger points in total are fixed and the trigger point i is corresponded to the t_i time and then the two arrays of the voltage signals from the coils are divided into 8192 sections. The sampling rate of the acquisition device is constant, that means the sampling interval dt is constant. Then the flux can be obtained from the integration of the voltage (V_j) numerically with software

$$\Delta\Phi_k(\theta) = -\int_{t_i}^{t_{i+16}} V_j dt \quad (i = 1 + 16k, \quad k = 0,1,2......511) \tag{2}$$

Every 16 encoder pulses are taken as an integral interval and 512 points of the integration value are acquired per cycle.

The coil was rotated by a servo motor precisely controlled using feedback from the encoder. The rotational stability can be monitored by the sampling interval dt and the size of the array for each group of the 16 TTL trigger points. It was observed that the rotational speed fluctuates around the set speed. The standard deviation of integral interval time was about 1.57E−4 s. For a coil with a large size and weight of about 150 kg, it can be considered as a stable rotation.

For a well designed and fabricated magnet, the high order harmonic is about 10^{-4} magnitude relative to the fundamental field. In analog bucking, the outer coil is used to measure the most dominant harmonic term. Two coils are connected in opposition to null the fundamental field allowing the full range of the data acquisition system to resolve the high order harmonic only. In reality, the coils cannot entirely null the fundamental field because of unavoidable mechanical errors in winding the two sets of coils. In order to both maintain a reasonable mechanical tolerance and null

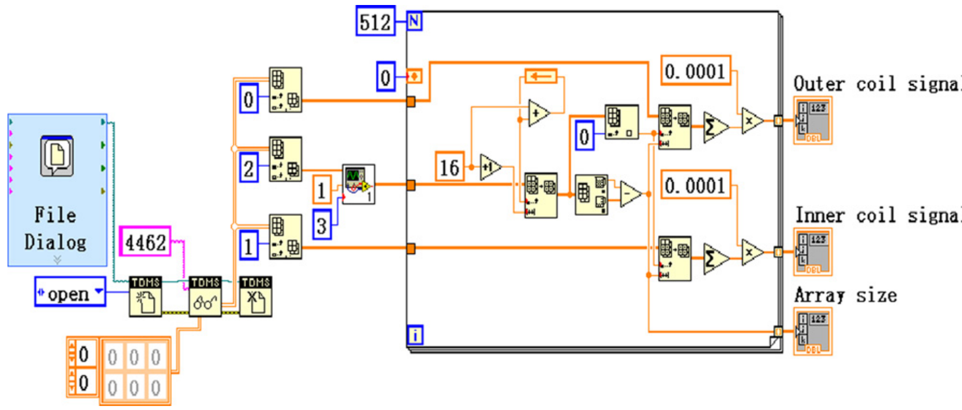

Fig. 5. Signal identify code.

Table 4
Systematic harmonic components before and after end chamfer and the magnetic center offset after end chamfer.

Current (A)	Not chamfer			Chamfer			Magnetic center offset (chamfer)	
	B_6/B_2	B_{10}/B_2	B_{14}/B_2	B_6/B_2	B_{10}/B_2	B_{14}/B_2	X_0 (mm)	Y_0 (mm)
260	4.55E−03	8.41E−04	5.38E−05	5.28E−05	1.08E−04	1.81E−05	−0.04	−0.33
400	4.94E−03	8.05E−04	4.96E−05	3.58E−04	7.31E−05	1.84E−05	−0.04	−0.34
1024	5.47E−03	7.55E−04	3.89E−05	8.85E−04	2.81E−05	2.28E−05	−0.03	−0.33
1600	5.80E−03	7.30E−04	3.97E−05	1.30E−03	5.07E−05	2.75E−05	−0.04	−0.31

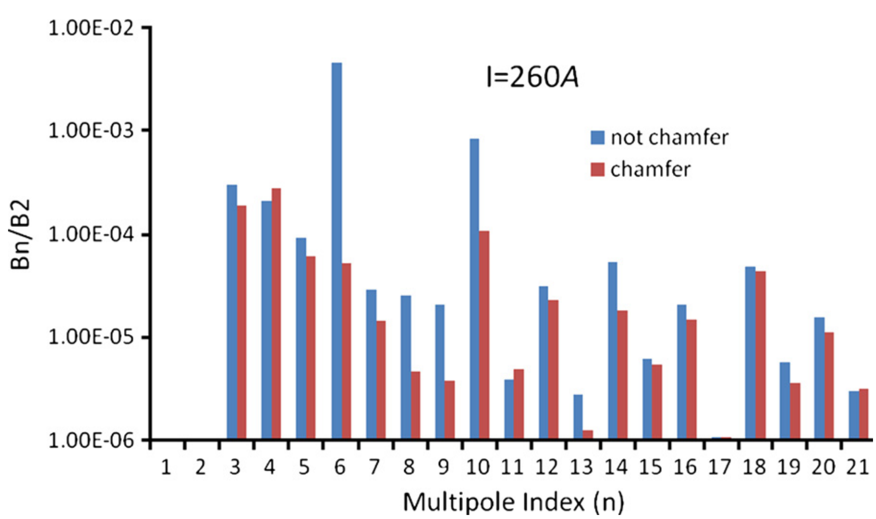

Fig. 6. High order harmonic components at current 260 A.

the fundamental field completely, the digital bucking technology has been used. Two separate coil signals are acquired by the PXI-4462 device at one time, a summing coefficient *f* is determined as 1.008 from a FFT analysis of the signals [13] in this measurement system to buck out the dipole and the quadrupole components. The bucked signal is then digitally constructed according to the following relation:

$$\Phi_{bucked}(\theta) = \Phi_{out}(\theta) - f\Phi_{in}(\theta) \quad (3)$$

where Φ_{out} and Φ_{in} are the flux signals from the outer and inner coil, respectively. The *f* is a real number and determined based on which fundamental fields are to be eliminated. To evaluate the residual level of them, a bucking ratio is computed [12]. Generally speaking, an acceptable value of bucking ratio is ≧100. For this measurement system, the bucking ratio is about 128.

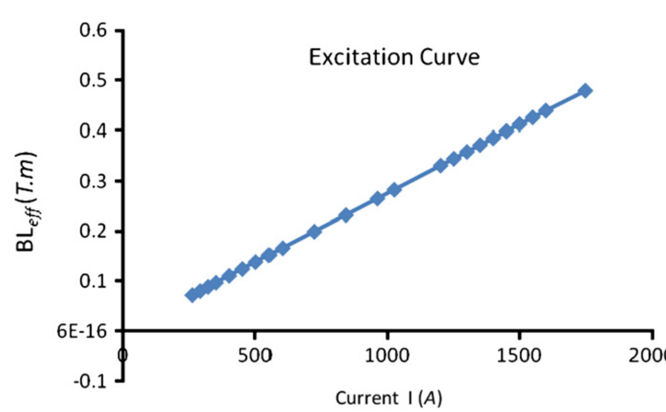

Fig. 7. Excitation curve of the magnet at the radius of 141 mm.

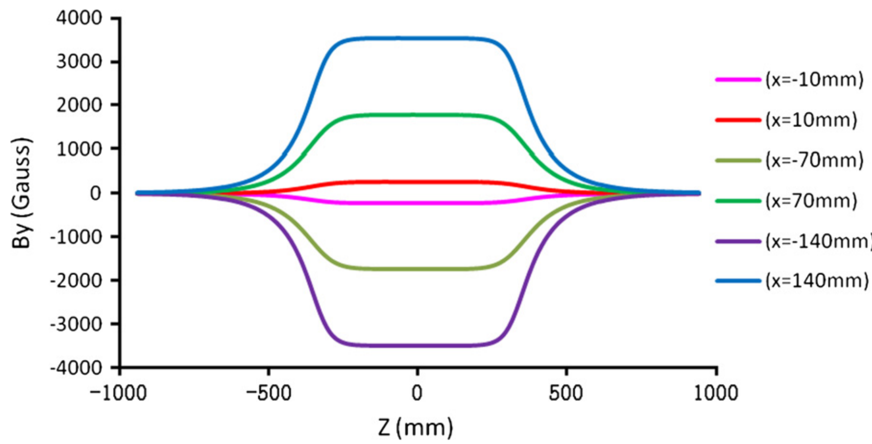

Fig. 8. Spatial distributions of the vertical component of the field B_y as function of the longitudinal coordinate z.

5. Measurement results and analysis

According to the CSNS/RCS physics requirements, the harmonic components have been measured at key currents $I=260$ A, 400 A, 1024 A, 1600 A before and after pole end chamfer. The reproducibility errors of the measured harmonics are less than 10^{-5}. The systematic harmonic components before and after pole end chamfer are shown in Table 4, the magnetic center offset after end chamfer are also listed in this Table. Fig. 6 shows all the high order harmonic fields at 260 A. Obviously, some of the harmonic terms are reduced very significantly after end chamfer.

Fig. 7 shows the excitation curve of the magnet at the radius of 141 mm. After actual measurement, the non-linearity of the excitation curve is about 9×10^{-3}, which is smaller than the requirements in Table 1. The reproducibility of the integrated field at different currents in different times is less than 2×10^{-4} and the magnetic field angle deviation is less than 0.5°.

Since the CSNS magnets have a high aspect ratio (inner diameter over magnet length), the contribution from magnet ends becomes significant [8]. The field distributions of the magnet are measured using the Hall probe on a 3-axis movable stage [7,16]. Fig. 8 shows the magnetic field distributions along z axial direction at medium plane ($y=0$ mm) at $I=261$ A. It can be seen that the field has a long extension along the z direction because of the fringe field. However the field at the $z=\pm940$ mm decreases to 0.4% of that at $z=0$ mm. For the 2 m long harmonic coil, it is enough to cover the overall effect of harmonic fields along the beam axis.

6. Conclusions

A novel harmonic coil measurement system has been developed, which is based on the perfect integration of dedicated algorithm and a dynamic signal acquisition device. It outperforms the existing PDI 5025 system when applied to continuous distributions of data in a broad input range and at high rate. After half year's operation, the DC magnetic field measurement of CSNS/RCS prototype quadrupole magnet was performed accurately and stably. It provides the valuable direction for the magnet design and pole end chamfer. The AC magnetic field measurement of the prototype quadrupole will be performed in the future.

Acknowledgment

The authors would like to thank all of the IHEP staff working on the magnetic field measurement.

References

[1] CSNS Design Report, June 2007.
[2] J.G. Wang, Phys. Rev. ST Accel. Beams 9 (2006) 122401.
[3] Y. Chen, J.Y. Tang, Phys. Rev. ST Accel. Beams 11 (2008) 032401.
[4] Yuan Chen, The study of fringe field effects of magnet in the synchrotron, Ph.D. Thesis, Institute of High Energy Physics Chinese Academy of Sciences, 2008.
[5] M. Yoshimoto, et al., IEEE Trans. Appl. Supercond. 18 (2) (2008) 301.
[6] A. Lazzaro, et al., Nucl. Instr. and Meth. A 591 (2008) 394.
[7] W. Chen et al., The Hall Probe Magnet Measurement Facility for BEPCII, in: Proceedings of the APAC 2004, Gyeongju, Korea, pp. 649–650.
[8] A.V. Fedotov, et al., EPAC (2000) 1492.
[9] WANG Sheng, et al., Lattice design for the BSNS rapid cycling synchrotron, HEP and NP 30 (Suppl. I) (2006) 123 in Chinese.
[10] CSNS/ACC Technical notice, CSNS-ACAP-TC-08-01.
[11] PDI 5025 Precision Digital Voltage Integrator, METROLAB Instruments SA, January 2000.
[12] Jack Tanabe, Iron dominated electromagnets design, fabrication, assembly and measurements, SLAC-R-754, June 2005.
[13] Animesh K. Jain, Measurements of field quality using harmonic coils, US Particle Accelerator School on Superconducting Accelerator Magnets, January 22–26, 2001, Houston, Texas, USA.
[14] Multifilar® Magnet Wire, MWS Wire Industries, ⟨http://www.mwswire.com/mfilar.htm⟩.
[15] NI 446x Specifications, National Instruments, Inc., December 2008.
[16] L. Li et al., Hall probe measurement of the CSNS/RCS prototype quadrupole magnet, Department Report, 2010.